

# Type-II band alignment in Si/Si<sub>1-x</sub>Ge<sub>x</sub> quantum wells from photoluminescence line shifts due to optically induced band-bending effects: Experiment and theory

T. Baier, U. Mantz, K. Thonke, and R. Sauer  
*Abteilung Halbleiterphysik, Universität Ulm, D-89069 Ulm, Germany*

F. Schäffler and H.-J. Herzog  
*Daimler-Benz AG, Forschungsinstitut Ulm, D-89013 Ulm, Germany*

(Received 11 July 1994)

We compare measured energy shifts of photoluminescence lines in Si/Si<sub>1-x</sub>Ge<sub>x</sub> quantum wells as a function of excitation power with theoretical calculations to conclude that the band alignment of the heterointerface is type II. Experimentally, we study molecular-beam-epitaxy-grown fully strained Si/Si<sub>1-x</sub>Ge<sub>x</sub> single quantum wells with Ge fractions from 10% to 36%. These show significant blueshifts of the luminescence at increasing excitation density. Theoretically, we calculate self-consistently transition energy changes taking into account band bending due to the photoinduced charge carriers. Only for type-II band alignment are the experimental and theoretical results compatible.

## I. INTRODUCTION

Nowadays fully strained Si<sub>1-x</sub>Ge<sub>x</sub> quantum wells (QWs) of high quality can be grown on silicon substrates for germanium fractions of up to  $\approx 36\%$ . Many experimental data are available but there is still a controversy on the conduction-band lineup in these systems. While it is clear that the alloy forms a well (type-I alignment) or a barrier (type-II alignment) for the electrons. Calculations of People and co-workers<sup>1,2</sup> and Van de Walle and Martin<sup>3</sup> indicate a type-I lineup for Ge fractions of up to 40% with a maximum conduction-band offset of 20 meV for  $x \approx 20\%$ . Northrop *et al.*<sup>4</sup> claim evidence for a type-I lineup for  $x = 25\%$  from photoluminescence (PL) measurements under high hydrostatic pressure. PL data of Xiao *et al.*<sup>5</sup> were interpreted so as to show type-I lineup for  $x \leq 35\%$ . Optical data of Fukatsu and Shiraki<sup>6</sup> were also taken as support for type-I lineup at  $x = 17\%$ .

Optically detected magnetic resonance measurements were interpreted as evidence for type-I arrangement for unrelaxed layers.<sup>7</sup> In contrast, calculations of Rieger and Vogl<sup>8</sup> yield a type-II lineup for all germanium fractions with the conduction-band offset growing linearly in  $x$  having a value of 30 meV at  $x \approx 40\%$ .

Earlier PL experiments of our group<sup>9</sup> on virtually undoped solid source molecular-beam-epitaxy- (MBE-) grown single quantum wells showed a strong blueshift of the QW emission lines as the excitation power was increased. From these data a type-II band alignment was derived using intuitive arguments. Excitation dependent QW emission energies were also observed by another group<sup>6</sup> on gas source MBE-grown samples. However, to our knowledge this effect has never been investigated systematically either on the experimental or on the theoretical side.

The present work expands our earlier studies theoretically and experimentally. The focus is on the effect of

optically induced carriers on the energy bands and the associated shifts in QW luminescence energies. A simple model is used and the numerical results are qualitatively compared to our experimental findings on several sets of solid source MBE-grown virtually undoped fully strained Si<sub>1-x</sub>Ge<sub>x</sub> single quantum wells on (100) Si substrates with various well widths and germanium fractions. The experimental data can be understood if a type-II band alignment is assumed. Band-bending effects are shown to be almost an order of magnitude larger than effects by band filling and excitonic corrections.

The paper is divided into six sections. Section I is this introduction. In Sec. II a Hartree-type model is set up which describes photoinduced carriers in a Si/Si<sub>x</sub>Ge<sub>1-x</sub> QW structure. The equations governing excitonic binding are introduced there also. In Sec. III numerical results are presented and interpreted. Our experimental data are presented in Sec. IV and a comparison to the predictions of our model is made. In Sec. V an estimate of the photoinduced carrier density is given and the effects of band filling are discussed. A summary and concluding remarks are given in Sec. VI.

## II. MODEL

In order to study band bending numerically in a self-consistent way we use a simple two-band model taking into account electrons and heavy holes. The calculations are performed for  $T=0$  K where only the lowest electron and hole states are occupied. In-plane gradients of the carrier densities and band-filling effects are neglected for the moment. The remaining motion of the carriers is described by two one-particle effective-mass Schrödinger equations,

$$\begin{aligned} H_i(p, z)\psi_i(z) &= \left[ p \frac{1}{2m(z)} p + V_i(z) \right] \psi_i(z) \\ &= E_i \psi_i(z), \end{aligned} \quad (1)$$

where  $i$  denotes either the valence ( $v$ ) or the conduction band ( $c$ ) and  $z$  is the growth direction. The carriers are assumed to move in the potential

$$V_i(z) = V_i^{\text{het}}(z) + \varphi(z), \quad (2)$$

where  $V_i^{\text{het}}$  is the quantum well potential caused by the band discontinuities and  $\varphi$  denotes the self-consistent Hartree potential caused by the electrostatic interaction of the charged carriers. Here exchange interactions of the carriers could principally be taken into account but are neglected due to the low carrier densities. In fact, calculations of Bauer and Ando<sup>10</sup> on electron hole plasmas in GaAs/Al<sub>x</sub>Ga<sub>1-x</sub>As quantum wells have shown only minor corrections to the transition energies for the maximum sheet carrier densities of  $n = 10^{11} \text{ cm}^{-2}$  considered here. Since in our case electrons and holes are spatially separated we expect the effects to be even smaller. The Hartree potential  $\varphi(z)$  is obtained from Poisson's equation,

$$\frac{d}{dz}\varepsilon(z)\frac{d}{dz}\varphi(z) = 4\pi e^2[n_c(z) - n_v(z)], \quad (3)$$

where  $\varepsilon(z)$  is the dielectric function, and  $n_c$  and  $n_v$  are the carrier densities determined by the normalized wave functions  $\psi_i(z)$ :

$$n_i(z) = n |\psi_i(z)|^2. \quad (4)$$

The sheet density of carriers  $n$  is treated as a parameter which is monotonously dependent on the experimental excitation density. Equations (1)–(4) together with appropriate boundary conditions fully determine the wave functions  $\psi_i(z)$  and the Hartree potential  $\varphi(z)$ . They can be solved iteratively.

So far, the possible formation of excitons from uncorrelated electrons and holes has been neglected. Excitonic binding leads to a lowering of the luminescence transition energy. The binding energy of an exciton is strongly dependent on the effective distance between the electron and the hole and thus is expected to depend also strongly on the self-consistent band bending. We evaluate excitonic corrections following Ref. 11 with the use of Ritz's variational principle. Our trial wave function reads

$$\psi(\varrho, z_c, z_v) = \psi_c(z_c)\psi_v(z_v)e^{-\alpha\varrho}e^{-\beta|z_c - z_v|}. \quad (5)$$

Here,  $z_c$  and  $z_v$  are the  $z$  coordinates of electrons and holes, respectively, and  $\varrho$  is the relative radial coordinate. The two parameters  $\alpha$  and  $\beta$  are used to minimize the energy functional

$$E(\alpha, \beta) = \frac{\langle \psi | H | \psi \rangle}{\langle \psi | \psi \rangle} \quad (6)$$

with the two-particle Hamiltonian

$$H = H_c(p_{c,z}, z_c) + p_{c||} \frac{1}{2m_{c||}} p_{c||} + H_v(p_{v,z}, z_v) + p_{v||} \frac{1}{2m_{v||}} p_{v||} - \frac{e^2}{\varepsilon \sqrt{\varrho^2 + |z_c - z_v|^2}}, \quad (7)$$

where the in-plane motion and the Coulombic two-particle interaction is included in addition to the effective

one-particle Hamiltonians. We have used a trial wave function which is separable in  $\varrho$ . Therefore the integrals over  $\varrho$  in Eq. (6) can approximately be expressed by an analytic formula. This greatly reduces the numerical expense. It also introduces an error which has been checked for the case of the hydrogen atom of varying dimension  $d$ . While the wave function is exact for  $d = 2$ , it leads to an error of 17% in the binding energy for  $d = 3$ . Since quantum well structures lead to more or less two-dimensional excitons we assume that the error in the excitonic correction of our calculated energies is negligible.

### III. NUMERICAL RESULTS

Figure 1 shows qualitatively the expected band bending (solid lines) and the wave functions (dashed lines) for a type-II quantum well system with nonvanishing carrier density. The separation of electrons and holes which leads to the Hartree potential (dotted line) causing the band bending is obvious. The electron ground state energy is lowered by the band bending due to the formation of two triangular wells. The hole ground state in turn is pushed even more towards the Si valence band, so that the total transition energy increases as the carrier density increases.

Figure 2 demonstrates this dependence quantitatively. It shows the change in the transition energy between carrier density  $n = 0$  and  $n = 10^{11} \text{ cm}^{-2}$  as a function of the conduction-band offset for a fixed valence-band offset of 200 meV, calculated for various well widths without excitonic correction. We note the following trends: (i) For both type-I and type-II alignments, a shift towards higher energies in the peak position occurs when the carrier density is increased. (ii) For small conduction-band offsets the upshift strongly depends on the actual size of the offset. (iii) In a type-II structure the upshift for a

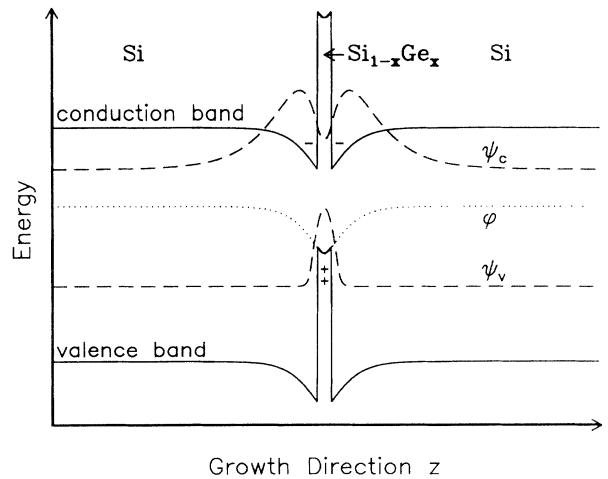


FIG. 1. Scheme of the band bending (full lines) and wave functions (dashed lines) under the presence of optically induced carriers for a type-II quantum well structure. The dotted line shows the electrostatic potential induced by the indicated charge separation. The step in the conduction band is exaggerated.

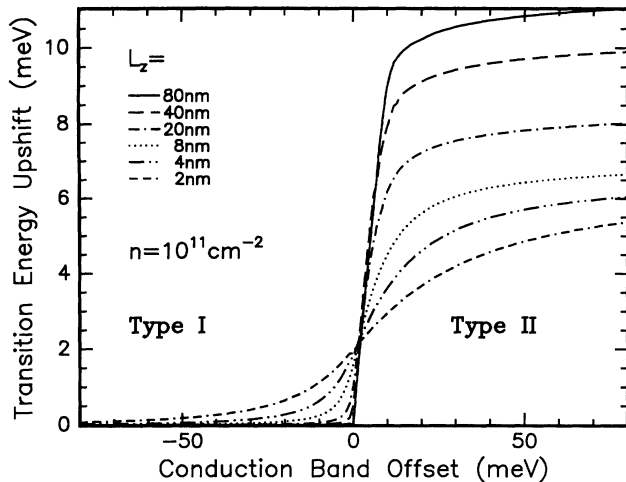


FIG. 2. Upshift of the optical transition energy of quantum wells vs the conduction-band offset due to a change in the carrier density from 0 to  $10^{11} \text{ cm}^{-2}$ . Different curves correspond to varying  $L_z$ .

fixed change in carrier density increases, as the well width increases whereas it decreases in a type-I structure. (iv) Band-bending effects are greatly reduced as the system becomes more type I.

All these observations can also be understood intuitively. From Fig. 1 it is clear that the species with higher localization in the well (here the holes) will be affected more by the Hartree potential. Since all energy levels are obviously pushed down, an increase in energy level separation occurs. This is true for a type-I and a type-II structure, thus explaining item (i). In a type-II structure an increase in the conduction-band offset will alter the electron wave function until the barrier has reached a height where essentially no electrons can penetrate into the barrier any longer. Thus a dependence of the peak shift on the conduction-band offset is only expected for small offsets as stated in item (ii). The feature (iii) is especially remarkable, since it *allows one to distinguish between type-I and type-II band alignment unambiguously*. The change in the peak shift as a function of the well width  $L_z$  changes the sign when going from type I to type II. This is also intuitively clear. In a type-I structure both electron and hole wave functions tend to become more alike as  $L_z$  is increased. Both approach the cosine-shaped ground state wave function of an infinitely deep rectangular QW. In this case charge separation and induced electric fields are reduced with growing  $L_z$  as stated in item (iv). In contrast, an increase of  $L_z$  in a type-II structure leads to an increase in the charge separation, which in turn leads to growing band-bending effects.

Figure 3 shows the excitonic corrections for carrier densities  $n = 0$  and  $n = 10^{11} \text{ cm}^{-2}$ , respectively. While the dependence of the excitonic binding energy for type-I band alignment on the carrier density is negligible, there is an increase of about 2 meV in the type-II system as  $n$  is increased from 0 to  $10^{11} \text{ cm}^{-2}$ . This effect counteracts the upshift of the transition energy due to charge accumulation. Since it is only a small correction, Fig.

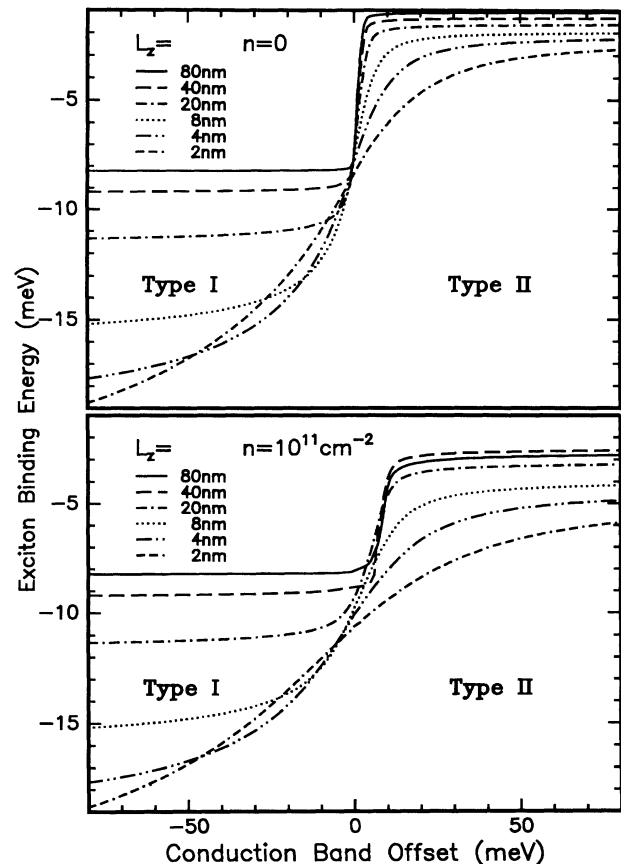


FIG. 3. Excitonic binding energy in the quantum well vs the conduction-band offset for sheet carrier density  $n = 0$  and  $n = 10^{11} \text{ cm}^{-2}$ .

2 describes the behavior of the system precisely enough also in the presence of excitonic effects. Nevertheless it is quite remarkable that a small change in the conduction-band offset from 0 to 10 meV dramatically lowers the excitonic binding energy.

#### IV. EXPERIMENTAL DATA AND DISCUSSION

Figure 4 shows typical series of photoluminescence spectra of Si/Si<sub>0.76</sub>Ge<sub>0.24</sub> single quantum wells recorded at two different excitation powers and at various temperatures. The narrow width of the depicted no-phonon (NP) emission lines at low temperature and the high luminescence outputs compared to the substrate luminescence (not shown) indicate that our samples are of extraordinarily good quality for a strained structure composed of indirect band gap materials. Note that the displayed energy intervals are quite narrow. The upshifts of the no-phonon lines due to the increase in excitation power are obvious. From the fact that the peak shifts are much larger than the peak broadening with increasing excitation power we conclude that the upshifts cannot be attributed to band-filling effects. We also exclude effects due to binding of the excitons to impurities or alloy fluctuations from the fact that the upshifts are basically

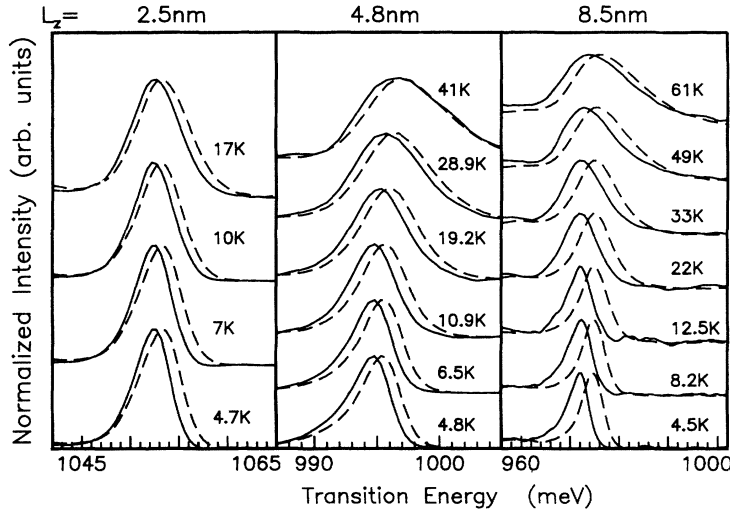


FIG. 4. Normalized no-phonon photoluminescence lines of a series of Si/Si<sub>0.76</sub>Ge<sub>0.24</sub> quantum wells with varying  $L_z$  for various temperatures. Solid lines correspond to an excitation power of  $\approx 0.2 \text{ W cm}^{-2}$ ; dashed curves correspond to  $\approx 0.4 \text{ W cm}^{-2}$ .

independent of temperature in the range up to 60 K. In PL measurements with an applied electric field on some PIN samples (not shown) we have found no shift of the QW luminescence energies within an error of 0.5 meV as a function of the applied voltage, thus excluding space charge effects from the surface. Therefore, we believe that band bending is the only reasonable explanation for the upshift.

Table I shows the experimentally observed shifts of the no-phonon PL lines for various single quantum wells, when the pumping laser power is increased from the PL detection limit to 100 mW. The samples were grown in five series with varying Ge fraction  $x$ . Within each series  $x$  was held constant while the well width  $L_z$  was varied. It is evident that the upshifts *increase* in each series with *increasing*  $L_z$ , except for the widest wells. The upshifts also increase with larger  $x$ . We interpret these observations within the results depicted in Fig. 2. We conclude that all samples must have a type-II band lineup since the upshifts grow with increasing  $L_z$ . If the band alignment were of type I, we would expect the upshifts to decrease with growing  $L_z$ . This is a qualitative argument which can also be understood intuitively as we have shown. It is not an argument based on the special numerics. The fact that the upshifts are dramatically dependent on  $x$  indicates that the conduction-band offset is small and that the system becomes more and more type II as  $x$  increases. The reason why the widest samples do not obey this trend, but show relatively small upshifts as compared to the narrower ones, might have two explanations. First, samples with wider QWs are known to be of minor quality, i.e., they incorporate a greater number of dislocations acting as nonradiative recombination centers compared to the narrow wells. This decreases the number of carriers in the quantum well and therefore the electric field induced by carrier separation. Second, it is also conceivable that in the case of wide wells the band bending has already reached its maximum for excitation levels below the PL detection limit. This is likely, since the detection limit is generally shifted to higher excitation powers with the lower quality of the wider well

samples.

In our experiments we observe a saturation of the peak shifts which we also expect to take place in our model. This is not a direct result of our calculations since the numerics used here fails for large charge densities when the type-II conduction-band barrier is pushed below the value of the conduction-band edge far away from the well, thus transforming the type-II system effectively into type I. A further increase in the charge density cannot alter the band structure beyond flattening, thus putting an upper limit to energy shifts associated with band bending.

TABLE I. Observed line shifts  $\Delta E$  as the excitation power is increased from  $P_{\min}$  to  $P_{\max} = 100 \text{ mW}$ . The excitation laser spot had a diameter of  $\approx 2 \text{ mm}$  except for the samples with  $x = 36\%$ , where the spot diameter was  $\approx 5 \text{ mm}$ .

$x$ (%)	$L_z$ (nm)	$P_{\min}$ ( $\mu\text{W}$ )	$\Delta E$ (meV)
10.0	2.5	370	1
10.0	10.0	370	4
10.0	20.0	370	7
18.5	1.1	10	<1
18.5	2.1	10	2
18.5	5.5	10	4
18.5	10.0	100	10
18.5	30.0	1000	<1
20.5	1.2	10	<1
20.5	1.8	1	3
20.5	3.5	1	4.5
20.5	250.0	1000	1
24.0	2.5	1	5
24.0	4.8	1	10
24.0	8.5	100	20
24.0	21.0	100	20
24.0	175.0	100	2
36.0	2.5	20	8
36.0	6.5	1900	21
36.0	13.0	5700	35
36.0	20.0	2700	34

## V. ESTIMATES OF CARRIER DENSITIES AND BAND FILLING

An upper limit of the photoinduced carrier density in the stationary state can be obtained by assuming that every photon incident on the sample creates an electron-hole pair. The stationary sheet carrier density can then be calculated by

$$n = \frac{P}{A} \frac{\tau}{h\nu}, \quad (8)$$

where  $P/A$  is the pump laser power per area,  $\tau$  is the carrier lifetime, and  $h\nu$  is the photon energy. Our experiments were performed with a maximum pump power of 100 mW delivered to a sample area of 4 mm<sup>2</sup> by photons with the wavelength 488 nm. By time resolved PL measurements we found carrier lifetimes of  $\tau \approx 0.5$   $\mu$ sec. Thus a maximum sheet carrier density of  $n = 3 \times 10^{12}$  cm<sup>-2</sup> is calculated. In reality a considerable fraction of light is reflected from the sample surface. Also, a considerable number of carriers recombine in the substrate, as can be seen from the photoluminescence spectra (not shown here). Thus the assumed carrier density of  $10^{11}$  cm<sup>-2</sup> in our numerical calculations is in reasonable agreement with the maximum carrier density estimated here.

The influence of band filling on the peak shift can be estimated by using the density of states of a two-dimensional hole gas which is present in the well,

$$\frac{dn}{dE} = \frac{m_{v||}}{\pi \hbar^2}. \quad (9)$$

Here  $dn$  is the number of states per area lying in the energy interval  $dE$  and  $m_{v||}$  is the in-plane hole mass, which is identical with the light hole mass  $m_{lh}$ . Thus the maximum peak shift  $\Delta E$  induced by a filling of  $\Delta n$  states per area amounts to

$$\Delta E = \frac{\pi \hbar^2}{m_{lh}} \Delta n. \quad (10)$$

An assumed filling of  $\Delta n = 10^{11}$  cm<sup>-2</sup> leads to an energy shift in the hole quasi-Fermi level of  $\Delta E = 1.6$  meV. A filling of conduction-band states can be neglected, since the in-plane electron mass is about  $6m_{lh}$  and, in addition, the lowest electron states are fourfold degenerate in the Si/Si<sub>1-x</sub>Ge<sub>x</sub> system. Thus in a type-II structure the line shifts due to band filling are almost an order of magnitude smaller than the shifts induced by band bending. In addition, our analysis shows that the peak shifts due to band-filling are independent of the well width  $L_z$ . So far, we assumed that only one hole subband is occupied. If at constant  $n$  higher subbands are being occupied as

the well width increases, the increase in the density of states leads to a reduction of band-filling effects. This is in contradiction to the experimentally observed increase in peak shift with growing  $L_z$ .

Our NP luminescence is not to be mistaken for the "localized exciton" NP luminescence, which in fact shifts due to band filling.<sup>12,13</sup> The latter effect occurs at very low excitation levels and is well resolved from our NP luminescence. We could only observe it in samples with  $x = 10\%$  and  $L_z \geq 10$  nm.

## VI. SUMMARY

Due to the long lifetimes of charged carriers in the indirect band gap materials Si and Si<sub>x</sub>Ge<sub>1-x</sub> a large number of carriers can be accumulated at low excitation levels in a standard PL experiment on QWs made from these materials. We have shown intuitively and by model calculations that the band bending induced by these carriers leads to a blueshift of the QW luminescence which increases with increasing well width if a type-II band alignment is assumed. We have also shown that, in contrast, for a type-I structure the blueshift should decrease with growing  $L_z$ . It turns out that excitonic corrections to the peak shift are unimportant. Experimentally, excitation dependent PL measurements on various Si/Si<sub>x</sub>Ge<sub>1-x</sub> single quantum wells were performed. The observed dependence of the blueshift on the well width is only compatible with band-bending effects in a type-II structure but not with a type-I structure or with band filling. Thus our experiments lead us to the conclusion that in our samples with  $10\% \leq x \leq 36\%$  the band alignment is type II.

To determine experimentally the conduction-band offset by photoluminescence from a series of samples as performed in Refs. 5 and 6, it is necessary to control well widths and Ge fractions to a high accuracy. Therefore the data of Fukatsu and Shiraki<sup>6</sup> can also be understood for a type-II alignment assuming a smaller excitonic binding energy and a slightly higher Si<sub>1-x</sub>Ge<sub>x</sub> band gap. The higher band gap could be explained by a variation in  $x$  of  $\approx 0.5\%$  in the reference sample.

In contrast, our analysis does not rest crucially on the exact knowledge of these growth parameters. Thus it is potentially more reliable than the studies cited above and our conclusions are contradictory to the results obtained there.

## ACKNOWLEDGMENT

We thank M. Wachter (Universität Ulm, Abteilung Halbleiterphysik) for his experimental assistance.

<sup>1</sup> R. People and J. C. Bean, Appl. Phys. Lett. **48**, 538 (1986).

<sup>2</sup> R. People, J. C. Bean, and D. V. Lang, in *Proceedings of the 18th International Conference on Physics of Semiconductors*, edited by O. Engström (World Scientific, Singapore,

1987), p. 767.

<sup>3</sup> C. G. Van de Walle and R. M. Martin, Phys. Rev. B **34**, 5261 (1986).

<sup>4</sup> G. A. Northrop, J. F. Morar, D. J. Wolford, and J. A.

- Bradley, *J. Vac. Sci. Technol. B* **10**, 2018 (1992).
- <sup>5</sup> X. Xiao, J. C. Sturm, L. C. Lenchyshyn, and M. L. W. Thewalt (unpublished).
- <sup>6</sup> S. Fukatsu and Y. Shiraki, *Appl. Phys. Lett.* **63**, 2378 (1993).
- <sup>7</sup> E. R. Glaser, T. A. Kennedy, D. J. Godbey, P. E. Thompson, K. L. Wang, and C. H. Chern, *Phys. Rev. B* **47**, 1305 (1993).
- <sup>8</sup> M. M. Rieger and P. Vogl, *Phys. Rev. B* **48**, 14 276 (1993).
- <sup>9</sup> M. Wachter, K. Thonke, R. Sauer, F. Schäffler, H.-J. Herzog, and E. Kasper, *Thin Solid Films* **222**, 10 (1992).
- <sup>10</sup> G. E. W. Bauer and T. Ando, *Phys. Rev. B* **34**, 1300 (1986).
- <sup>11</sup> G. Bastard, E. E. Mendez, L. L. Chang, and L. Esaki, *Phys. Rev. B* **26**, 1974 (1982).
- <sup>12</sup> L. C. Lenchyshyn, M. L. W. Thewalt, J. C. Sturm, P. V. Schwartz, N. L. Rowell, J.-P. Noël, and D. C. Houghton, *J. Electron. Mater.* **22**, 233 (1993).
- <sup>13</sup> L. C. Lenchyshyn, M. L. W. Thewalt, D. C. Houghton, J.-P. Noël, N. L. Rowell, J. C. Sturm, and X. Xiao, *Phys. Rev. B* **47**, 16 655 (1993).